J. Fluid Mech. (2006), *vol.* 551, *pp.* 31–48.
doi:10.1017/S0022112005008244 Printed in the United Kingdom

The motion of a point vortex through gaps in walls

By DARREN CROWDY AND JONATHAN MARSHALL

[1]Department of Mathematics, Imperial College of Science, Technology and Medicine, 180 Queen's Gate, London, SW7 2AZ, UK

(Received 4 February 2005 and in revised form 2 September 2005)

New analytical techniques for studying the motion of a point vortex in fluid domains bounded by straight walls having an arbitrary number of gaps are presented. By exploiting explicit formulae for the Kirchhoff–Routh path function in multiply connected circular domains, combined with a novel construction of conformal mappings from such circular domains to multiply connected slit domains, the governing Hamiltonians for the motion of a point vortex in a number of physically interesting fluid regions involving walls with gaps are derived. The vortex trajectories in several illustrative cases are computed. These examples include finding the vortex paths around a chain of islands sitting off an infinite coastline, around islands in an unbounded ocean and around a sequence of islands situated between two headlands.

1. Introduction

In a recent paper, Johnson & McDonald (2004*b*) have studied the problem of vortex motion near a wall punctured by a single gap. With no gap present, it is a well-known result of classical fluid dynamics that a point vortex near an infinite straight wall travels at constant speed parallel to the wall. This result is most easily understood by considering the celebrated 'method of images' (Milne-Thomson 1972) in which the streamline condition on the wall is enforced by placing an 'image' point vortex of opposite circulation at the reflected point in the wall. When a gap is present, Johnson & McDonald (2004*b*) find that, if the point vortex starts off far from the gap at a distance of less than half the gap width from the wall, it will travel along the wall until it eventually penetrates the gap; otherwise, its trajectory will dip towards the gap but will not go through it.

In a natural extension of this single-gap problem, Johnson & McDonald (2005) have also examined the more general case of vortex motion near an impenetrable barrier with multiple gaps. They analyse the case of point-vortex motion near a wall with two gaps in detail and are able to produce a formula for the governing Hamiltonian in analytical form. This is done by combining the method of Schwarz–Christoffel mapping with elements of elliptic function theory. In addition to the analytical treatment of the point-vortex problem, Johnson & McDonald (2005) go on to combine conformal mapping methods with well-developed contour dynamics codes to accurately compute the numerical solution for the motion of vortex patches in the same fluid domain. Such flow scenarios are of interest since they occur in a wide range of geophysical situations such as the interaction of Mediterranean salt lenses ('Meddies') with seamounts in the Canary basin (Dewar 2002), or the collision of North Brazil Current rings with the islands of the Caribbean (Simmons & Nof

2002), as well as in a variety of other geophysical applications (DiGiacomo & Holt 2001; Nof 1995; Simmons & Nof 2000). The problem of vortex motion in multiply connected fluid domains is therefore of great interest.

On this subject, Crowdy & Marshall (2005*a*) have presented a new analytical framework for finding the Kirchhoff–Routh path functions, or Hamiltonians, governing the motion of N vortices in general multiply connected domains in the special case when all the circulations around the impenetrable obstacles (or 'islands') are zero. In this special case, they find explicit analytical formulae for the path functions for point-vortex motion in the canonical class of bounded *circular domains* (defined in the next section) of arbitrary finite connectivity. The analysis makes use of a special transcendental function denoted $\omega(\zeta, \gamma)$. When combined with transformation properties of the path functions under conformal mapping as first unveiled by Lin (1941) in the multiply connected case, the general formalism developed by Crowdy & Marshall (2005*a*) can be used to study flow domains of interest in applications. Indeed, Crowdy & Marshall (2005*b*) have used the new formalism to study point-vortex motion around an arbitrary finite number of circular islands, thereby extending an earlier analysis of Johnson & McDonald (2004*a*) who studied the case of two circular islands. The treatment of circular islands turns out to be particularly tractable because the conformal mapping from the bounded circular domains considered by Crowdy & Marshall (2005*a*) to the unbounded fluid domains exterior to a collection of circular islands has a simple analytical form (it is just a Möbius map).

The purpose of this paper is to show how to extend the general formalism presented by Crowdy & Marshall (2005*a*) to find an analytical framework in which to study the problem of point-vortex motion in multiply connected domains bounded by straight walls with multiple gaps (we shall refer to such domains as multiply connected slit domains). To do so requires the derivation of explicit formulae for conformal mappings from the bounded circular domains considered by Crowdy & Marshall (2005*a*) to these multiply connected slit domains. The key result here is to show that the required conformal mappings can be constructed using exactly the same transcendental function $\omega(\zeta, \gamma)$ used by Crowdy & Marshall (2005*a*) to construct the point-vortex Hamiltonians. This is a surprising result. Having found the formulae for such conformal mappings, the vortex trajectories in various flow domains of physical interest are presented in the single-vortex case.

In this way, the present paper complements and extends the recent work of Johnson & McDonald (2004*b*) and Johnson & McDonald (2005). An important result of the latter work is that the motion of the centroid of a finite-area vortex patch that is close to circular is, in many instances, close to that of a point vortex of the same total circulation, even in the presence of boundary effects. This provides further motivation for the present study since it is evidence of the usefulness of being able to readily compute trajectories, within the point-vortex approximation, of vortices in geometrically complicated domains.

2. Mathematical formulation

Let D_ζ be a bounded circular domain with the outer boundary given by $|\zeta| = 1$. A circular domain is defined to be a domain whose boundaries are all circles. Henceforth, the circle $|\zeta| = 1$ will be denoted C_0. Let M be a non-negative integer and let the boundaries of M enclosed circular disks be denoted $\{C_j | j = 1, \ldots, M\}$. $M = 0$ corresponds to the simply connected case where there are no enclosed circular disks. Let the radius of circle C_j be $q_j \in \mathbb{R}$ and let its centre be at $\zeta = \delta_j \in \mathbb{C}$.

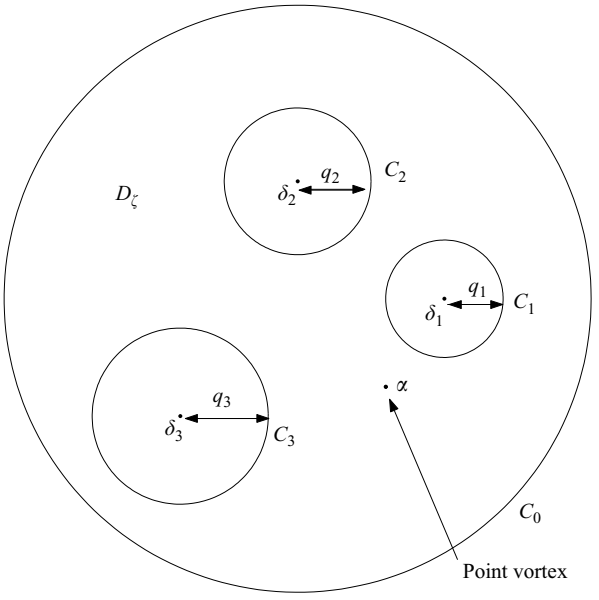

FIGURE 1. Schematic illustrating the circular pre-image domain D_ζ consisting of the unit ζ-circle with M smaller circular disks excised. The boundaries of the interior circular disks are denoted $\{C_j | j = 1, \ldots, M\}$. Their centres and radii are denoted $\{\delta_j, q_j | j = 1, \ldots, M\}$. The point vortex is taken to be at the point $\zeta = \alpha$.

Such a domain is $(M + 1)$-connected. Figure 1 illustrates an example of a quadruply connected circular domain.

Let $W(\zeta, \alpha)$ be the complex potential associated with an incompressible flow in D_ζ which is irrotational except for a single point-vortex singularity at $\zeta = \alpha$. Assume also that all the circulations around the M enclosed circular islands are zero. $W(\zeta, \alpha)$ must be analytic (but not necessarily single-valued) everywhere in D_ζ except for a logarithmic singularity at $\zeta = \alpha$ corresponding to the point vortex. It must also be such that

$$\mathrm{Im}[W(\zeta, \alpha)] = 0 \quad \text{on } C_0, \tag{2.1}$$

and

$$\mathrm{Im}[W(\zeta, \alpha)] = \beta_j(t) \quad \text{on } C_j, \quad j = 1, \ldots, M, \tag{2.2}$$

where the functions $\beta_j(t)$ depend possibly on time, but not space. Conditions (2.1) and (2.2) ensure that all flow boundaries are streamlines. The choice (2.1) provides a normalization which uniquely determines $W(\zeta, \alpha)$. The functions $\{\beta_j(t) | j = 1, \ldots, M\}$ are determined (essentially through Kelvin's circulation theorem) by the zero-circulation conditions around the islands.

It is demonstrated in Crowdy & Marshall (2005*a*) that an explicit formula for the complex potential $W(\zeta, \alpha)$ satisfying all the conditions above is

$$W(\zeta, \alpha) = -\frac{\mathrm{i}}{4\pi} \log \left(\frac{\omega(\zeta, \alpha)\overline{\omega}(\zeta^{-1}, \alpha^{-1})}{\omega(\zeta, \bar{\alpha}^{-1})\overline{\omega}(\zeta^{-1}, \overline{\alpha})} \right) \tag{2.3}$$

where ω and $\overline{\omega}$ are two transcendental functions defined in Crowdy & Marshall (2005*a*) by a pair of infinite products and dependent only on the parameters $\{q_j, \delta_j | j = 1, \ldots, M\}$ determining the circular domain D_ζ. Equation (2.3) is the complex potential corresponding to a point vortex of unit circulation. Let ψ be

the streamfunction associated with the flow. Then

$$\psi = \mathrm{Im}[W(\zeta,\alpha)] = -\frac{1}{4\pi}\log\left|\frac{\omega(\zeta,\alpha)\overline{\omega}(\zeta^{-1},\alpha^{-1})}{\omega(\zeta,\bar{\alpha}^{-1})\overline{\omega}(\zeta^{-1},\overline{\alpha})}\right|. \tag{2.4}$$

Now let $H^{(\zeta)}(\alpha,\bar{\alpha})$ denote the Hamiltonian (or Kirchhoff–Routh path function) for the motion of the vortex in D_ζ. It is shown in Crowdy & Marshall (2005*a*) that a formula for $H^{(\zeta)}(\alpha,\bar{\alpha})$ is

$$H^{(\zeta)}(\alpha,\bar{\alpha}) = -\frac{\Gamma^2}{8\pi}\log\left|\frac{1}{\alpha^2}\frac{\omega'(\alpha,\alpha)\overline{\omega}'(\alpha^{-1},\alpha^{-1})}{\omega(\alpha,\overline{\alpha}^{-1})\overline{\omega}(\alpha^{-1},\overline{\alpha})}\right|, \tag{2.5}$$

where the functions ω' and $\overline{\omega}'$ are also defined in Crowdy & Marshall (2005*a*). Equation (2.5) gives an explicit formula for the Hamiltonian of a single vortex in D_ζ.

In order to find the Hamiltonian for motion in domains that are more complicated than the bounded circular domains of figure 1, it is useful to employ a result of Lin (1941) showing how the Hamiltonian $H^{(\zeta)}(\alpha,\bar{\alpha})$ transforms under arbitrary conformal mapping of the domain D_ζ. Indeed, if D_ζ maps to a domain D_z by means of a one-to-one conformal map $z=z(\zeta)$, then the Hamiltonian $H^{(z)}(z_\alpha,\bar{z}_\alpha)$ in the image domain D_z is

$$H^{(z)}(z_\alpha,\bar{z}_\alpha) = H^{(\zeta)}(\alpha,\bar{\alpha}) + \frac{\Gamma^2}{4\pi}\log\left|\frac{\mathrm{d}z(\alpha)}{\mathrm{d}\zeta}\right| \tag{2.6}$$

where $z_\alpha = z(\alpha)$ and where superscripts on H annotate the respective complex planes in which H is the relevant Hamiltonian. Explicitly, by combining (2.5) and (2.6), this takes the form

$$H^{(z)}(z_\alpha,\bar{z}_\alpha) = -\frac{\Gamma^2}{8\pi}\log\left|\frac{1}{\alpha^2}\frac{\omega'(\alpha,\alpha)\overline{\omega}'(\alpha^{-1},\alpha^{-1})}{\omega(\alpha,\overline{\alpha}^{-1})\overline{\omega}(\alpha^{-1},\overline{\alpha})}\left(\frac{\mathrm{d}z(\alpha)}{\mathrm{d}\zeta}\right)^{-2}\right| \tag{2.7}$$

where it should be recalled that the one-to-one conformal mapping $z=z(\zeta)$ is invertible so that, in principle, ζ can be written as a function of z, i.e. $\zeta=\zeta(z)$, or as is more relevant for the formula (2.7), $\alpha=\alpha(z_\alpha)$.

If the vortex is moving in an unbounded domain where the circulations around all islands are required to be zero, (2.7) must be altered slightly. First, let $z(\zeta)$ be the conformal mapping from D_ζ to the unbounded flow region D_z. In order that the image domain is unbounded, there must be a point in D_ζ, denoted ζ_∞, such that $z(\zeta)$ has a simple pole there. In Crowdy & Marshall (2005*b*) it is shown that the general form of the Hamiltonian (in a conformally mapped z-plane) for vortex motion in this case is

$$H^{(z)}(z_\alpha,\bar{z}_\alpha) = -\frac{\Gamma^2}{8\pi}\log\left|\frac{\omega'(\alpha,\alpha)\overline{\omega}'(\alpha^{-1},\alpha^{-1})\omega^2(\alpha,\bar{\zeta}_\infty^{-1})\overline{\omega}^2(\alpha^{-1},\bar{\zeta}_\infty)}{\alpha^2\omega(\alpha,\overline{\alpha}^{-1})\overline{\omega}(\alpha^{-1},\overline{\alpha})\omega^2(\alpha,\zeta_\infty)\overline{\omega}^2(\alpha^{-1},\zeta_\infty^{-1})}\left(\frac{\mathrm{d}z(\alpha)}{\mathrm{d}\zeta}\right)^{-2}\right| \tag{2.8}$$

where, again, $z_\alpha = z(\alpha)$.

3. Conformal mapping to slit domains

To study the motion of a vortex through gaps in walls it is clearly necessary to find conformal mappings $z(\zeta)$ from a circular domain D_ζ to the physical flow region of interest for use in (2.7) and (2.8). The surprising fact is that conformal mappings to such slit domains can be constructed using the same special function $\omega(\zeta,\gamma)$ already used in (2.7) and (2.8). Thus, the special function ω enters the present analysis in two

distinct ways: both in the construction of $H^{(\zeta)}$ in the ζ-plane and in the construction of the map $z(\zeta)$ taking D_ζ to D_z.

The key conformal mapping to be exploited in all the subsequent examples is given by the simple form

$$z(\zeta) = R\frac{\omega(\zeta, \gamma_1)}{\omega(\zeta, \gamma_2)}, \tag{3.1}$$

where $R \in \mathbb{C}$ is a complex constant and γ_1 and γ_2 are taken to be two distinct points on the unit ζ-circle. The map (3.1) has some fortuituous properties. First, it maps $\zeta = \gamma_1$ to $z = 0$ and $\zeta = \gamma_2$ to $z = \infty$ in the physical plane. It can further be shown that it takes the unit ζ-circle to an infinite straight line passing through the origin. It also maps each of the interior circles $\{C_j | j = 1, \ldots, M\}$ to a finite-length radial slit on rays emanating from the origin $z = 0$. Appendix A features some details, based on the transformation properties of the special function $\omega(\zeta, \gamma)$ given in Crowdy & Marshall (2005*a*), of how these properties of (3.1) can be demonstrated. The map (3.1) will be a basic tool in the construction of all the conformal mappings needed in the examples to follow.

4. Examples

We will now exploit (3.1) to present examples of the motion of a point vortex around various geometrical arrangements of straight walls having gaps. In the geophysical context of oceanic eddy motion, infinite walls have an interpretation as coastlines, or headlands, while finite-length walls can be interpreted as modelling long, extended islands.

We restrict attention to the motion of a single point vortex (although the formulae for the Kirchhoff–Routh path functions derived by Crowdy & Marshall (2005*a*) apply more generally to the multi-vortex problem). It will always be assumed that the point vortex approaches the island clusters from infinity and that there are no imposed background flows. Therefore, the flow around the islands is initially trivial and all round-island circulations are initially zero. By Kelvin's circulation theorem, these circulations remain zero at later times – a circumstance automatically encoded in the formulae for the Hamiltonians just discussed. The motion is completely integrable – the contours of the (conserved) Hamiltonian give the point-vortex trajectories. In the following examples, explicit formulae for the Hamiltonian are first constructed and the trajectories found by plotting its level lines. As in Crowdy & Marshall (2005*b*), the infinite products defining the function $\omega(\zeta, \gamma)$ were truncated at level three (keeping all maps up to level three and omitting all higher level maps). To check the accuracy of the truncation, several of the calculations are performed at a higher level of truncation to ensure that the results are acceptably close.

4.1. *Walls off an infinite coastline*

The problem of the North Brazil current rings travelling along the Brazilian coastline to eventually negotiate the island cluster known as the Lesser Antilles motivates consideration of the situation in which a collection of finite-length walls are situated off an infinite coastline. Simmons & Nof (2002) consider models of precisely this kind (but with different governing equations). We take the imaginary axis in the z-plane to represent the coastline and consider various distributions of finite-length walls off this coastline in the right-half-plane. This is the domain D_z. Given a distribution of M finite-length walls in D_z, the geometrical arrangement of the M circles $\{C_j | j = 1, \ldots, M\}$ characterizing the pre-image domain D_ζ must be determined.

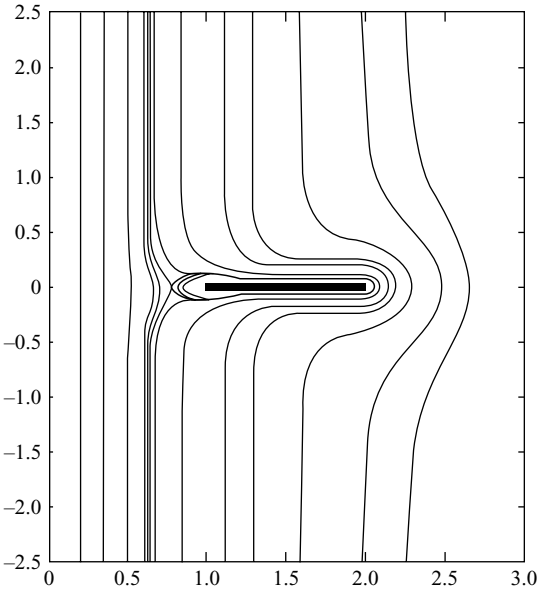

FIGURE 2. Distribution of trajectories for a single vortex in the presence of a unit-length slit situated at unit distance from a coastline.

The conformal mappings from circular domains to slit domains of this type are given by mappings of the form (3.1). Making the choices

$$\gamma_1 = 1, \quad \gamma_2 = -1, \quad R = -1, \tag{4.1}$$

then $\zeta = 1$ maps to $z = 0$, $\zeta = -1$ maps to $z = \infty$ while the rest of the unit ζ-circle maps to the whole of the imaginary z-axis (i.e. the infinite coastline) with interior points of D_ζ mapping to points in the right-half-z-plane. For a sequence of M finite walls aligned along the positive real axis in the physical plane, the sequence of pre-image circles $\{C_j | j = 1, \ldots, M\}$ corresponding to these walls will all be centred on the real ζ-axis. The centres and radii of these pre-image circles are determined by the choices of the end-point positions of the slits in D_z. Let a_j and $b_j > a_j$ be the (specified) end points of the slit on the positive real z-axis corresponding to the image of the circle C_j. Then the system of $2M$ equations to be solved for the $2M$ real parameters $\{q_j, \delta_j | j = 1, \ldots, M\}$ is given by

$$z(\delta_j + q_j) = a_j \quad \text{and} \quad z(\delta_j - q_j) = b_j, \quad j = 1, \ldots, M. \tag{4.2}$$

These nonlinear equations are readily solved using Newton's method.

Figure 2 shows the distribution of trajectories for point-vortex motion around a single unit-length island situated unit distance off an infinite coastline. In this case the flow domain is doubly connected so, without loss of generality, the domain D_ζ can be taken to be the annulus $\rho < |\zeta| < 1$ (so that we have taken $\delta_1 = 0$ and $q_1 = \rho$). As shown explicitly by Crowdy & Marshall (2005*b*), in such a case, the function $\omega(\zeta, \gamma)$ is given by

$$\omega(\zeta, \gamma) = -\gamma C^{-2} P(\zeta/\gamma, \rho) \tag{4.3}$$

where

$$P(\zeta, \rho) = (1 - \zeta) \prod_{k=1}^{\infty} (1 - \rho^{2k}\zeta)(1 - \rho^{2k}\zeta^{-1}) \tag{4.4}$$

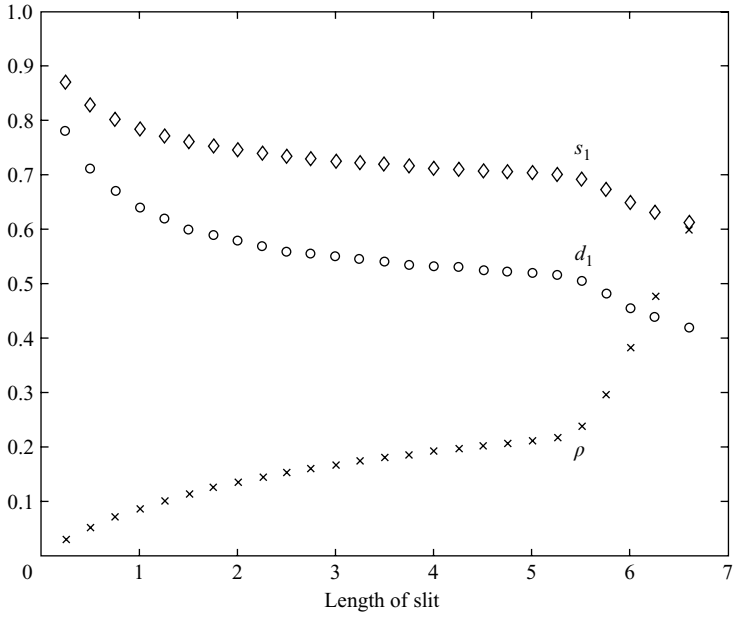

FIGURE 3. Graph of ρ, s_1 and d_1 against length of slit for the case of a single slit sitting off an infinite coastline. ρ is the radius of the inner circle of the annulus D_ζ, s_1 is the distance of the separatrix trajectory from the coastline far up-coast of the island and d_1 is the point between the coastline and the island at which the two parts of the separatrix trajectory cross each other.

and $C = \prod_{k=1}(1-\rho^{2k})$, so that the first transformation in the sequence (4.10) below is

$$\zeta_1(\zeta) = -R\frac{P(\zeta,\rho)}{P(-\zeta,\rho)}. \tag{4.5}$$

When far away from the island, the vortex travels along trajectories that are nearly parallel to the coastline since the vortex has yet to feel the influence of the island and simply evolves under the effects of its 'image' reflected in the coastline. As the vortex gets closer to the island, there are two possible eventualities: either it passes through the gap between the island and the coastline or it diverts around the island avoiding the gap altogether. Let s_1 denote the distance from the coastline (far up-coast of the island) of the separatrix trajectory which divides the two possible sets of trajectories. A quantity of practical interest is how this critical distance s_1 from the coastline depends on the island's length and position. Such quantities are readily computed using the formulation above. For example, let us fix one end of the island to be at unit distance from the coastline and consider islands of differing lengths. Figure 3 shows graphs of the following quantities as functions of the length of the island: the value of s_1 just defined, the position d_1 (between 0 and 1) on the real axis at which two parts of the separatrix trajectory cross each other and the parameter ρ.

To illustrate the flexibility of the methods, figure 4 shows the case of two unit-length islands; the one nearest to the coastline is unit distance from it and is separated from the second island by distance 2.5. In this example there are now two circles, C_1 and C_2, inside the unit ζ-disk because D_z is now triply connected.

There is no restriction on how many offshore islands can be studied using this approach. Figure 5 shows just the critical trajectories for the case of three, four and

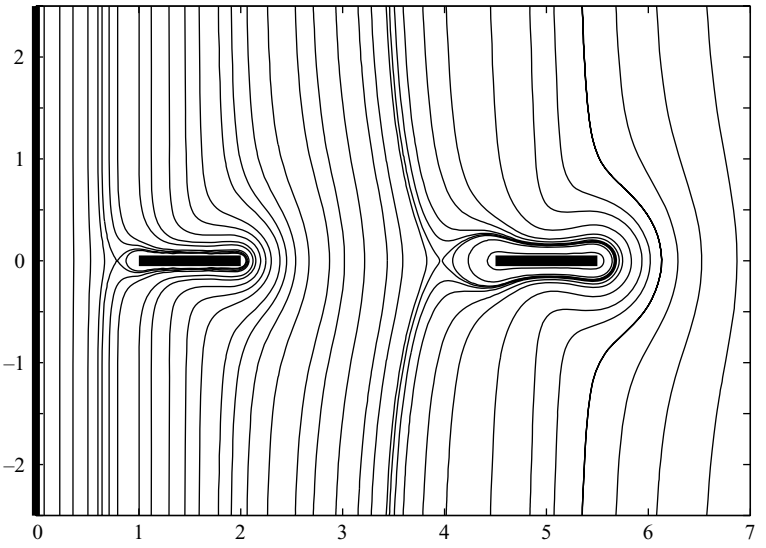

FIGURE 4. Trajectories for a single vortex in the presence of two unit-length slits separated by distance $d = 2.5$. The slit nearest to the coastline is unit distance from it. The far-field distances of the critical trajectories from the coastline are 0.64 and 3.41.

five unit-length islands off a coastline, again separated from the coastline, and from each other, by unit distance. Such trajectories are obtained simply by adding more pre-image circles in the circular pre-image domain D_ζ and solving a system of nonlinear equations to ascertain the relevant centres and radii of the circles $\{C_j | j = 1, \ldots, M\}$.

The offshore islands need not necessarily lie along the real axis. Figure 6 shows the distribution of trajectories around two unit-length islands off a coastline each making an angle of $\pi/6$ to the positive real axis. Again, one makes use of the general mapping formula (3.1) – it is simply required to solve a small system of nonlinear equations for the centres and radii of the two pre-image circles C_1 and C_2 corresponding to the two offshore islands.

When the slit images of all the inner circles are aligned along the positive real z-axis it can be argued, on grounds of symmetry, that the pre-image circles must similarly be centred on the real axis in the ζ-plane so that the equations to be solved are precisely those given in (4.2). However, when the slit images are not aligned with the positive real axis it is no longer known *a priori* which two points on any pre-image circle map to the end points of the slit in the z-plane. Let the end points of the slit in the z-plane be

$$a_j e^{i\phi_j}, \quad b_j e^{i\phi_j}, \tag{4.6}$$

where the real parameters a_j, b_j and ϕ_j are specified. Let the two pre-image points on C_j corresponding to the end points of the slit be

$$\delta_j + q_j e^{ir_j}, \quad \delta_j + q_j e^{is_j}, \tag{4.7}$$

where r_j and s_j are real parameters. The latter parameters must be found as part of the solution. The required additional equations are provided by the fact that, at these pre-image points, the derivative of the conformal mapping must vanish since the argument of the image undergoes a change of 2π as ζ passes through them. Thus, the equations to be solved in this case for the parameters $\{q_j, \delta_j | j = 1, \ldots, M\}$, as

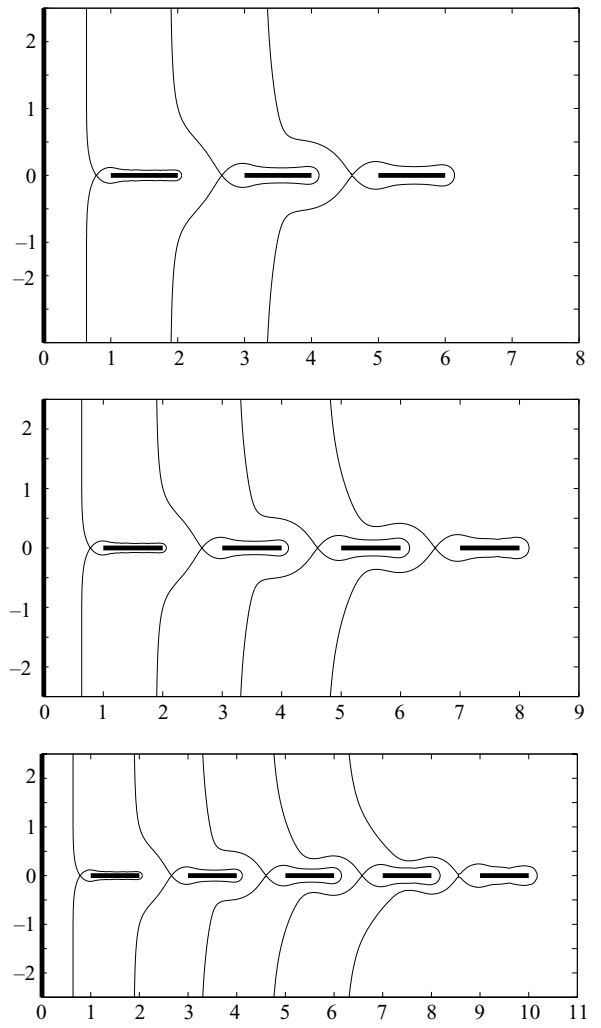

FIGURE 5. Critical trajectories for a single vortex in the presence of three, four and five unit-length slits separated by distance $d=1$ sitting off an infinite coastline. The far-field distances from the coastline of the critical trajectories are 0.64, 1.89 and 3.29 (3 slits), 0.64, 1.88, 3.25 and 4.70 (4 slits) and 0.64, 1.88, 3.25, 4.70 and 6.12 (5 slits).

well as the subsidiary parameters $\{r_j, s_j | j = 1, \ldots, M\}$, are

$$\left.\begin{aligned} |z(\delta_j + q_j \mathrm{e}^{\mathrm{i}r_j})| &= a_j, \left|\frac{\mathrm{d}z}{\mathrm{d}\zeta}(\delta_j + q_j \mathrm{e}^{\mathrm{i}r_j})\right| = 0, \\ |z(\delta_j + q_j \mathrm{e}^{\mathrm{i}s_j})| &= b_j, \left|\frac{\mathrm{d}z}{\mathrm{d}\zeta}(\delta_j + q_j \mathrm{e}^{\mathrm{i}s_j})\right| = 0, \end{aligned}\right\} \tag{4.8}$$

together with the real equation

$$\phi_j = \arg[-1] + \tfrac{1}{2}\arg\big[-\beta_j(1,-1)\big] \tag{4.9}$$

which derives from a general formula, in terms of the conformal mapping parameters appearing in (3.1), for the angle made by the slit (corresponding to the image of C_j) with the positive real z-axis. See Appendix A for further details of this general

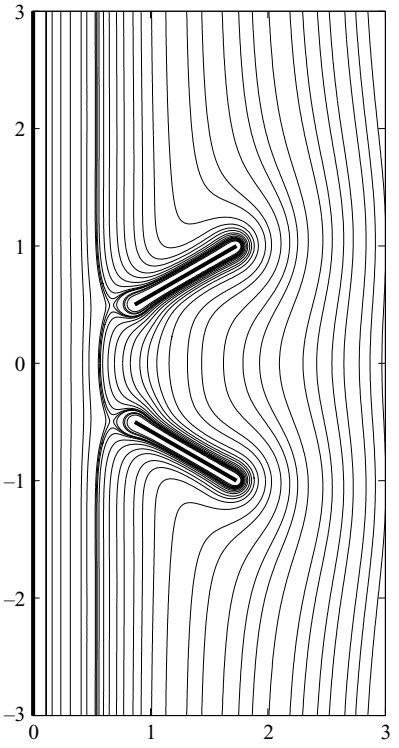

FIGURE 6. Trajectories for two slits of unit length making angles of $\pm\pi/6$ with the horizontal axis.

formula. Note that (4.8) and (4.9) represent five real equations for the five real unknowns, i.e. $\mathrm{Re}[\delta_j]$, $\mathrm{Im}[\delta_j]$, q_j, r_j and s_j.

4.2. *Flow past a flat plate above a wall*

Elcrat, Hu & Miller (1997) have exploited the doubly connected Schwarz–Christoffel formula to study the flow past objects, such as an inclined flat plate, in an infinite channel (modelling a wind tunnel) including examples where the upper wall of the channel is far from the object. Such a configuration is a special case of the situation just considered. Figure 7 shows the critical vortex trajectories around a unit-length flat plate inclined at various angles to the lower wall (i.e. this was the 'coastline' in the examples of the previous section, but we have now rotated the figures so that this infinite boundary is horizontal in order to more closely resemble the lower wall of a wind tunnel). In figure 7, the end of the finite-length slit closest to the wall is taken to be at $\mathrm{e}^{\mathrm{i}(\pi-\theta)}$ where θ is taken to have the values $4\pi/10$, $3\pi/10$, $2\pi/10$ and $\pi/10$. The slit mappings developed here can be considered as special cases of doubly connected Schwarz–Christoffel mappings but they do not require the usual Schwarz–Christoffel mapping formulae given in Elcrat *et al.* (1997) for their construction. Johnson & McDonald (2005) also make use of Schwarz–Christoffel mapping in their studies of point vortex motion past an infinite wall with two gaps. It should also be pointed out that, since this flow region is doubly connected, in principle it is possible to include the effects of background flows and non-zero circulation around the flat plate as in Elcrat *et al.* (1997).

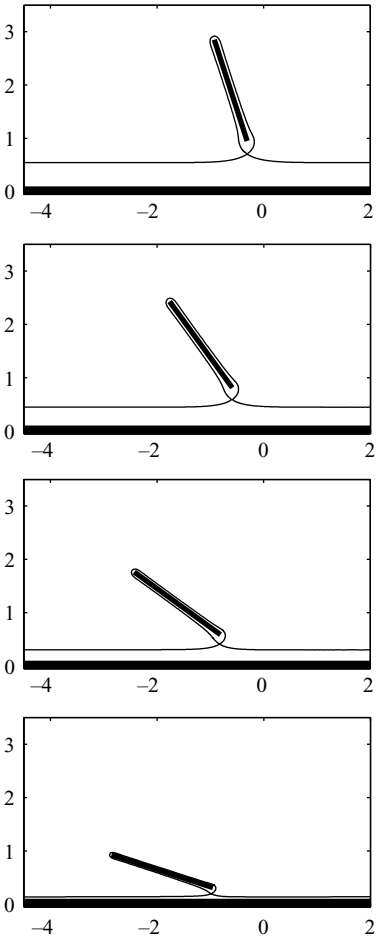

FIGURE 7. Critical trajectories for a finite flat plate making angles of $4\pi/10$, $3\pi/10$, $2\pi/10$ and $\pi/10$ with a wall.

4.3. *Walls in an unbounded ocean*

Now consider the case where the walls are not of infinite length but where several finite-length walls are placed in a line, with gaps between them, in an unbounded ocean. A conformal map from a circular region D_ζ must be found. Its construction is given by a composition of conformal mappings which includes the new mapping (3.1). The sequence of mappings is

$$\left.\begin{aligned} \zeta_1(\zeta) &= R\frac{\omega(\zeta,1)}{\omega(\zeta,-1)}, \\ \zeta_2(\zeta_1) &= \frac{1-\zeta_1}{1+\zeta_1}, \\ \zeta_3(\zeta_2) &= \frac{1}{4}\left(\frac{1}{\zeta_2}+\zeta_2\right), \end{aligned}\right\} \tag{4.10}$$

where R is now assumed to be real (and, in fact, negative) and all the circles $\{C_j | j = 1, \ldots, M\}$ are taken to be centred on the real ζ-axis. A schematic illustrating

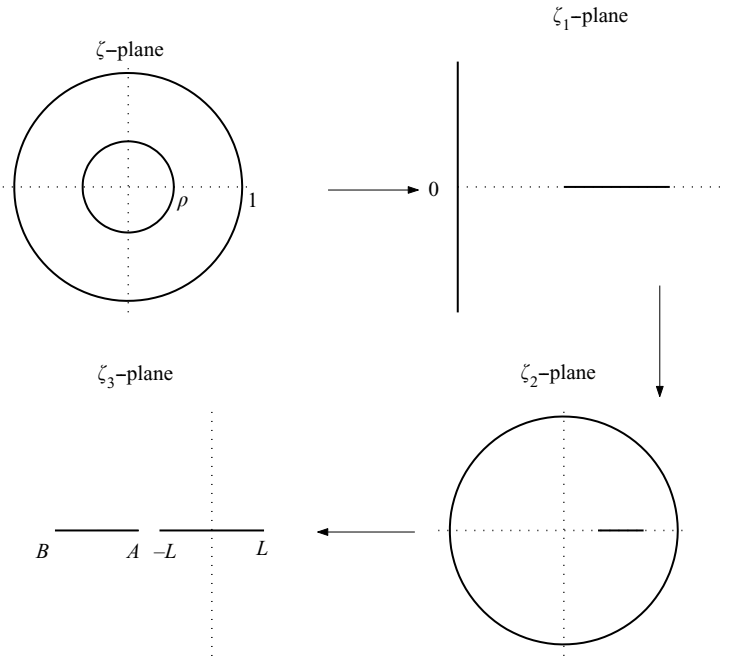

FIGURE 8. Schematic showing the composition of conformal mappings (4.10) to two slits in an unbounded ζ_3-plane.

this composition of mappings in the special case of a doubly connected region is shown in figure 8. D_ζ can be taken to be the annulus $\rho < |\zeta| < 1$. The first mapping takes this annular region to the right-half-plane cut by a finite slit along the real ζ_1-axis, exactly as in § 4.1. The second Möbius mapping takes this region back to the unit ζ_2-circle similarly cut inside by a finite slit along the real axis. The third Joukowski mapping maps the interior of the unit ζ_2-circle to the whole of the ζ_3-plane exterior to two finite slits along the real ζ_3-axis. Note that if the pre-image region contains additional circles (centred on the real ζ-axis) then the same sequence of mappings (modified only by use of the relevant choice of ω in the mapping $\zeta_1(\zeta)$) will produce additional finite slits along the real ζ_3-axis. Note that the sequence of mappings (4.10) always maps the unit circle to a finite slit between $\pm 1/2$ on the real ζ_3-axis. The ζ_3-plane can be taken to correspond to the required physical z-plane.

For example, consider the case of two such walls. The unbounded fluid region exterior to the two slits is a doubly connected region. The image of the unit circle is the slit between $\pm 1/2$ on the real z-axis and the values of the two real parameters R and ρ can be chosen in order to specify the end points of the second slit corresponding to the image of $|\zeta| = \rho$.

Since this is an unbounded flow it is necessary to use formula (2.8) for the Hamiltonians. This means that the circulation around each of the islands is zero. It is straightforward to identify the interior point ζ_∞ mapping to $z = \infty$ by inverting the sequence of mappings (4.10). With ζ_∞ known, the form of the Hamiltonian (2.8) is then used to compute the trajectories.

Figure 9 shows typical point-vortex trajectories around two equal-length islands, separated by unit distance, in an unbounded ocean. R and ρ are chosen so that the end points of the island corresponding to $|\zeta| = \rho$ are at $-3/2$ and $-5/2$. It is

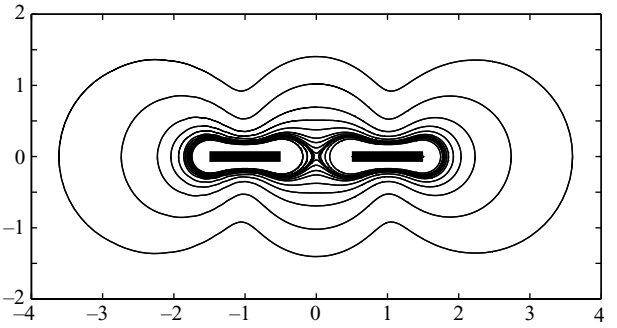

FIGURE 9. Vortex trajectories around two unit-length slits, separated by unit distance, in an unbounded ocean.

clear that there are separatrix streamlines between regions of closed streamlines that encircle each island individually and regions of closed streamlines encircling both islands. Similar vortex trajectories for greater numbers of islands can be computed in a similar way by changing the number of pre-image circles $\{C_j | j = 1, \ldots, M\}$ and using the appropriate function $\omega(\zeta, \gamma)$ in (4.10).

4.4. *Two headlands with intermediate islands*

Johnson & McDonald (2005) have discussed the general problem of vortex motion around a chain of islands sitting between two headlands. In Johnson & McDonald (2004*b*) the problem of point-vortex motion through a single gap in an infinite straight wall is solved explicitly while the generalization to two gaps is solved in Johnson & McDonald (2005). We now show how to solve the general case of any number of gaps.

It is necessary to find a conformal mapping from D_ζ to the fluid region exterior to an infinite wall with a number of gaps. Again, this follows from the composition of mappings (4.10) but with an additional Möbius mapping (of the final ζ_3-plane) having a simple pole on the slit between $\pm 1/2$. This maps the unit ζ-circle to two headlands (both going off to infinity) with two finite end points on the real axis.

It is natural to consider first the case of a symmetrically disposed chain of islands between the two headlands. It is possible to verify that provided we choose

$$R = -1 \tag{4.11}$$

in the sequence (4.10) and take the circles $\{C_j | j = 1, \ldots, M\}$ to be reflectionally symmetric about both the real and imaginary ζ-axes then any two points $\zeta = \pm a$ will map to two equal and opposite points in the ζ_3-plane, i.e.

$$\zeta_3(-a) = -\zeta_3(a). \tag{4.12}$$

Thus the final image of the sequence (4.10) is a distribution of slits on the real ζ_3-axis which are symmetrically disposed with respect to the origin $\zeta_3 = 0$. To ensure that the image of the unit circle (on which $\psi = 0$) corresponds to the two headlands, consider an additional Mobius mapping of the ζ_3-plane given by

$$z(\zeta_3) = \frac{1}{2\zeta_3}. \tag{4.13}$$

The slit corresponding to the unit ζ-circle now maps to two (symmetric) headlands going through the point at infinity with end points at ± 1 and corresponds to a

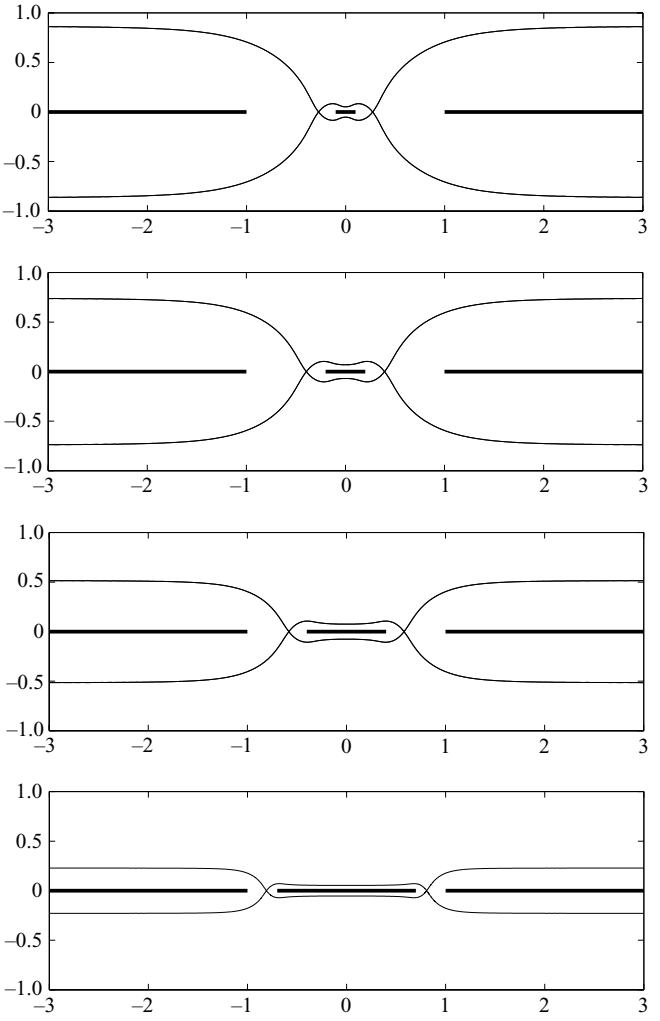

FIGURE 10. An infinite wall with two equal gaps of length 0.2, 0.4, 0.8 and 1.4. The edges of the infinite walls are at ± 1. This figure should be compared with figure 7 of Johnson & McDonald (2005).

boundary on which $\psi = 0$. As discussed by Johnson & McDonald (2005), the fact that the two headlands have the same value of ψ corresponds to there being no net flux between the two sides of the domain separated by the punctured wall, a situation that is certainly satisfied if both sides of the punctured wall are closed basins. The images of all the other interior circles are symmetrically disposed slits between the two headlands. The final composed form of the mapping takes the simple form

$$z(\zeta) = \frac{\omega^2(\zeta, -1) - \omega^2(\zeta, 1)}{\omega^2(\zeta, -1) + \omega^2(\zeta, 1)}. \tag{4.14}$$

In figure 10 we take the wall with a gap between $-1 < x < 1$, as considered by Johnson & McDonald (2004*b*), and examine the effect of 'growing' another segment of wall at the centre of the gap at $x = 0$. We consider here the case of a wall with two

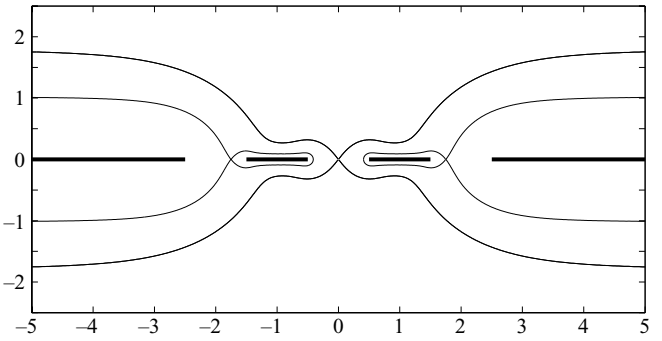

FIGURE 11. Critical trajectories for vortex motion around an infinite wall with three gaps. If the vortex is closer than unit distance from the wall, it travels through the first gap, if it is between unit distance and distance 1.8 from the wall it travels through the middle gap. If it is further than 1.8 from the wall, it travels through neither gap. The walls between the headlands are taken to be between −1.5 and −0.5 and between 0.5 and 1.5. The headlands extend up to −2.5 and 2.5.

symmetric gaps. The function $\omega(\zeta, \gamma)$ is again given by (4.3) so that the first mapping $\zeta_1(\zeta)$ is again given by (4.5).

When the new segment of wall is small, the critical trajectories tend to $y = 1$ as $x \to \pm\infty$. This is consistent with the results of Johnson & McDonald (2004*b*) where it is shown that vortices that start off less than half the gap width from the wall penetrate the gap. As the added segment of wall grows larger, the far-field height of the critical trajectory decreases. As might be expected, when the added segment of wall is almost filling the original gap so that the two gaps are now very small and well-separated, the critical trajectories have moved very close to the wall. As the gaps vanish, the trajectories degenerate to straight lines parallel to the wall.

Johnson & McDonald (2005) include graphs showing the through-gap flux as a function of the length of the intermediate island. It is not necessary to reproduce such graphs here, only to mention that explicit analytical formulae exist for the inter-island fluxes within the present formulation and these are recorded, for completeness, in Appendix B.

There is no difficulty in adding more gaps. Figure 11 shows the critical vortex trajectories in the case of a wall with three symmetric gaps. The fluid domain is now triply connected and the circular pre-image domain is the unit circle with two smaller circular disks excised. There are now two distinct critical trajectories. If the vortex far away from the gaps is within approximately unit distance from the wall it will travel through the first gap in the wall and return whence it came (but on the other side of the wall); if it is farther from the wall, but closer than a distance of approximately 1.8, it will travel through the central gap in the wall and also return whence it came. If it is any farther from the wall it will not penetrate any of the gaps. It by-passes all of them and eventually returns to the trajectory it would have followed in the absence of any gaps.

Finally, if a non-symmetric distribution of walls between the headlands is of interest, one proceeds in the same manner as above but now the distribution of pre-image circles $\{C_j | j = 1, \ldots, M\}$ will not necessarily be reflectionally symmetric about both real and imaginary ζ-axes. All circles should, nevertheless, still be centred on the real axis. Their centres and radii are found by solving a system of equations analogous to (4.2).

5. Discussion

This paper has demonstrated the efficacy and flexibility of a new analytical method for calculating the motion of a point vortex in fluid domains bounded by straight walls with multiple gaps. By combining analytical expressions for the Kirchhoff–Routh path function in multiply connected circular pre-image domains D_ζ with a transformation property of this function under conformal mapping to a multiply connected slit domain D_z, the single-vortex motion around a variety of different island configurations has been considered. The conformal mappings have themselves been constructed by strategic use of the conformal mapping (3.1).

The formulation presented above is very general and allows a large variety of interesting flow domains to be treated. However, there are a number of physical features still to be incorporated into the analytical formulation and these matters are currently under investigation. First, it is important to be able to incorporate background flows (e.g. uniform flows at infinity). The difficulty is then to find the complex potential, $W_B(z)$ say, having the appropriate singularity at physical infinity and satisfying all the streamline conditions on the various boundaries. It is also desirable to be able to include the case where the round-island circulations are not necessarily zero but fixed (by Kelvin's circulation theorem) to be some non-zero value throughout the motion. A generalized formulation is needed to incorporate this case. It should be noted that, in the doubly connected case, the incorporation of background flows and non-zero round-island circulations has already been performed (see e.g. Johnson & McDonald 2004*a*).

Another extension is to distributed vorticity. While attention has been restricted here to the motion of a single point vortex, the formulation also provides explicit formulae for the Hamiltonians relevant to the general N-vortex problem in the same domains. Thus, one idea for modelling distributed vorticity is to use the 'vortex cluster' model in which a collection of point vortices is chosen to model a vortical region. Dewar (2002) has employed this idea in modelling geophysical flows. Another model is that of a uniform vortex patch. While the preceding formulae for the Hamiltonians are no longer relevant to this case, certain aspects of the conformal mapping ideas may be of use: Johnson & McDonald (2004*b*) and Johnson & McDonald (2005) have shown how the well-developed numerical codes of contour dynamics (e.g. Dritschel 1988) can be strategically combined with elements of conformal mapping theory to accurately compute the motion of vortex patches around topography. So far, these only seem to have been applied to simply and doubly connected regions. However, the methods involve finding an irrotational correction to a vortical flow computed using the usual free-space Green's function (on use of regular contour dynamics codes). These irrotational corrections can be conveniently computed using conformal mappings from circular pre-image regions to the flow domain of interest and by making use of fast Fourier transforms. We fully expect that such methods can similarly be employed to higher connected regions using conformal mapping techniques from the multiply connected circular domains in this paper. Wegmann (2001) has shown, for example, the efficacy of a method of 'successive conjugation' in solving very general classes of Riemann–Hilbert problems on such multiply connected circular domains of the type considered here.

The efficacy of our method has been demonstrated by a series of examples. It should be pointed out, however, that we have proceeded under the assumption that the infinite products defining the functions ω and $\overline{\omega}$ converge. In fact, these products do not converge for all choices of the parameters $\{q_j, \delta_j | j = 1, \ldots, M\}$ – broadly speaking, their convergence depends on the distribution of circles $\{C_j | j = 1, \ldots, M\}$

in the pre-image plane. If the circles are 'well-separated' (in a sense that will be left imprecise here) then good convergence is assured. There is a large region of the parameter space $\{q_j, \delta_j | j = 1, \ldots, M\}$ where the convergence is completely adequate for practical purposes, as we have demonstrated by example. This region of parameter space is large enough to capture all of the physically interesting fluid domains investigated herein.

J. S. M. acknowledges the support of an EPSRC studentship. The authors thank Dr N. Robb McDonald for providing a preprint of Johnson & McDonald (2005).

Appendix A. Properties of the function (3.1)

Full details of the properties of the function $\omega(\zeta, \gamma)$ can be found in Crowdy & Marshall (2005*a*) and, in what follows, we adopt the notation used there. These properties can be used to demonstrate that the function (3.1) behaves in the manner described in § 3. In this Appendix, we briefly indicate how this can be done (without giving full details of the manipulations involved) and present the final form of some useful formulae (from Crowdy & Marshall 2005*a*) needed in the present paper.

First, the function $\omega(\zeta, \gamma)$ has a simple zero when $\zeta = \gamma$. This immediately implies that (3.1) has a simple zero at $\zeta = \gamma_1$ and a simple pole at $\zeta = \gamma_2$. Next, it can be shown using transformation properties of $\omega(\zeta, \gamma)$ given in Crowdy & Marshall (2005*a*) that (3.1) has constant argument on all the circles $\{C_j | j = 0, 1, \ldots, M\}$ (this can be done by considering the complex conjugate of (3.1) for values of ζ on the circles $\{C_j | j = 0, 1, \ldots, M\}$ and showing that they are inversely proportional to (3.1) on these circles). Since (3.1) has a pole and a zero on the unit circle, the image of the unit circle under this map is therefore an infinite straight line going through the origin and infinity while the image of each interior circle $\{C_j | j = 1, \ldots, M\}$ is a finite radial segment. An explicit formula for the angles made by the straight line image of the unit circle to the positive real axis can be shown (again, using the transformation properties of $\omega(\zeta, \gamma)$) to be

$$\arg[R] - \frac{1}{2}\arg\left[\frac{\gamma_2}{\gamma_1}\right] \quad \text{and} \quad \arg[R] - \frac{1}{2}\arg\left[\frac{\gamma_2}{\gamma_1}\right] + \pi \tag{A 1}$$

(where these differ simply by π). The angle to the positive real axis made by the finite slit image of circle C_j is

$$\arg[R] + \frac{1}{2}\arg\left[\frac{\gamma_1}{\gamma_2}\beta_j(\gamma_1, \gamma_2)\right] \tag{A 2}$$

where

$$\beta_j(\gamma_1, \gamma_2) = \prod_{\theta_k} \frac{(\gamma_1 - \theta_k(B_j))(\gamma_2 - \theta_k(A_j))}{(\gamma_1 - \theta_k(A_j))(\gamma_2 - \theta_k(B_j))}. \tag{A 3}$$

As explained in Crowdy & Marshall (2005*a*), the product defining β_j is taken over all Möbius mappings θ_k which do not have a (positive or negative) power of θ_j on the right-hand end while A_j and B_j are the two fixed points of the mapping θ_j so that they are the two roots of the quadratic equation $\zeta = \theta_j(\zeta)$. It is then possible to write

$$\frac{\theta_j(\zeta) - B_j}{\theta_j(\zeta) - A_j} = \mu_j e^{i\kappa_j} \frac{\zeta - B_j}{\zeta - A_j} \tag{A 4}$$

where μ_j, κ_j are real. The two roots A_j and B_j are distinguished by the fact that $|\mu_j| < 1$.

Appendix B. Inter-island fluxes

A useful result, derived in detail in Crowdy & Marshall (2005*a*), is a formula for the inter-island fluxes. Let $\mathscr{F}_{ij}$ denote the flux between the islands corresponding to circles C_i and C_j. Then, when the point vortex is at position $\zeta = \alpha$, this inter-island flux is given by the formula

$$\mathscr{F}_{ij} = -\frac{1}{4\pi} \log \frac{\beta_i(\bar{\alpha}, \alpha^{-1})}{\beta_j(\bar{\alpha}, \alpha^{-1})} \tag{B 1}$$

where β_i is given in (A 3) and it is understood that $\beta_0 = 1$ while if i (or j) is between 1 and M an expression for β_i (or β_j) follows from (A 3).

REFERENCES

Crowdy, D. G. & Marshall, J. S. 2005*a* Analytical formulae for the Kirchhoff-Routh path function in multiply connected domains. *Proc. R. Soc. Lond.* A **461**, 2477–2501.

Crowdy, D. G. & Marshall, J. S. 2005*b* On the motion of a point vortex around multiple circular islands. *Phys. Fluids* **17**, 056602.

Dewar, W. K. 2002 Baroclinic eddy interaction with isolated topography. *J. Phys Oceanogr.* **32**, 2789–2805.

DiGiacomo, P. M. & Holt, B. 2001 Satellite observations of small coastal ocean eddies in the Southern California Bight. *J. Geophy. Res.* **106**, 22521–22544.

Dritschel, D. G. 1988 Contour surgery: a topological reconnection scheme for extended contour integrations using contour dynamics. *J. Comput. Phys.* **77**, 240–266.

Elcrat, A. R., Hu, C. & Miller, K. G. 1997 Equilibrium configurations of point vortices for channel flows past interior obstacles. *Eur. J. Mech.* B/*Fluids* **16**, 277–292.

Johnson, E. R. & McDonald, R. N. 2004*a* The motion of a vortex near two circular cylinders. *Proc. R. Soc. Lond* A **460**,939–954.

Johnson, E. R. & McDonald, R. N. 2004*b* The motion of a vortex near a gap in a wall. *Phys. Fluids* **16**, 462–469.

Johnson, E. R. & McDonald, R. N. 2005 Vortices near barriers with multiple gaps. *J. Fluid Mech.* **531**, 335–358.

Lin, C. C. 1941 On the motion of vortices in two dimensions – II. Some further investigations on the Kirchhoff-Routh function. *Proc. Natl. Acad. Sci.* **27**, 575–577.

Milne-Thomson, L. M. 1972 *Theoretical Hydrodynamics*, 5th Edn. Macmillan.

Nehari, Z. *Conformal Mapping*. McGraw-Hill.

Nof, D. 1995 Choked flows from the Pacific to the Indian Ocean. *J. Phys. Oceanogr.* **25**, 1369.

Simmons, H. L. & Nof, D. 2000 Islands as eddy splitters. *J. Mar. Res.* **58**, 919–956.

Simmons, H. L. & Nof, D. 2002 The squeezing of eddies through gaps. *J. Phys. Oceanogr.* **32**, 314.

Wegmann, R. 2001 Constructive solution of a certain class of Riemann-Hilbert problems on multiply connected circular regions. *J. Comput. Appl. Maths.* **130**, 139–161.